Clays and Clay Minerals, Vol. 27, No. 5, pp. 339–348, 1979.

A MÖSSBAUER INVESTIGATION OF GLAUCONITE AND ITS GEOLOGICAL SIGNIFICANCE

D. M. McConchie,[1] J. B. Ward,[2] V. H. McCann,[3] and D. W. Lewis[4]

Abstract—Mössbauer spectra of 9 glauconite samples from Upper Cretaceous and Lower Tertiary strata in the South Island of New Zealand contain a broad shoulder due to low intensity absorption continuous between 1.0 and 2.5 mm/sec when the absorber is at room temperature; the shoulder is absent, and sharp peaks are apparent in spectra taken with the absorber at 80°K. The data suggest that electron transfer occurs between adjacent Fe^{3+} and Fe^{2+} ions at room temperature. The low temperature spectra indicate that all Fe in the glauconites is in octahedral coordination. Fe^{3+} and Fe^{2+} ions occur in both cis and trans sites; Fe^{3+} shows a strong preference for cis sites whereas Fe^{2+} shows an even stronger preference for trans sites.

The partially variable oxidation state of Fe in glauconite is interpreted in terms of a geochemical model for glauconitization of a degraded or incomplete progenitor phyllosilicate. The model involves exchange of Fe^{2+} for other cations which temporarily stabilize the progenitor, followed by Fe^{2+}–Fe^{3+} charge transfer reactions. Each reaction results from the system's tendency towards equilibrium. The model is supported by the observation that artificially leached glauconite increases both its Fe^{3+} and its Fe^{2+} content when placed in a solution containing Fe^{2+} as the only Fe ion present.

Key Words—Genesis, Glauconite, Iron oxidation, Mössbauer spectroscopy.

INTRODUCTION

The Mössbauer technique uses nuclear gamma resonance to produce absorption spectra which are sensitive to interactions between the nucleus and the extranuclear electric and magnetic fields. In its most basic form, the technique indicates the relative occupancies of different lattice sites by absorber atoms in different oxidation states, the presence of certain defects or distortions in the crystal structure, and the variability (if any) in the oxidation state of the absorber atoms. This paper amplifies earlier studies by Mössbauer analysis of the sedimentary mineral glauconite (cf. Rolf *et al.*, 1977; Rozenson and Heller-Kallai, 1978).

In this paper the term glauconite is restricted to greenish iron- and potassium-rich hydrated aluminophyllosilicates with 2:1 layer lattices; there may be a high proportion of expandable layers, but the nonexpandable components must be illitic (McRae, 1972). The presence of glauconite has been widely used as an indicator of paleoenvironments, and the conditions under which it forms have been summarized by many authors (e.g., Cloud, 1955; Burst, 1958a, 1958b; McRae, 1972) although the chemistry of glauconite genesis remains poorly understood. In this paper explanations for some of the chemical aspects of glauconite genesis, based on Mössbauer studies of selected New Zealand glauconites, are proposed.

EXPERIMENTAL

Sample collection, analysis, and classification

All samples were obtained from Upper Cretaceous and Lower Tertiary formations in the South Island of New Zealand (see Figure 1). A range of morphological, crystallographic, and compositional varieties of glauconite was selected (see Table 1) from an original collection representing 142 localities (McConchie, 1978). Approximately 1 kg of each sample was disaggregated in warm water and wet sieved to retain the size fraction between 0.125 mm and 1.0 mm. The use of a Frantz Isodynamic Magnetic Separator, followed by the manual removal of contaminants, produced concentrates containing only glauconite grains.

The morphology of the glauconite grains was determined using a binocular microscope, and their crystallographic properties were studied with a Philips X-ray powder diffractometer using oriented mounts; no contaminants were detected in any of the samples. Both the proportion of layers in the glauconite crystallites with a variable basal spacing (% expandable layers—see McRae, 1972) and the disorder coefficient (DC) were determined. The disorder coefficient (McConchie, 1978) is a measure of crystallographic disorder and is defined as $DC = (\tau\, b)/(h - b)$; where τ is the half-height line width of the 10-Å reflection measured in $^{o}2\theta$ using an oriented sample fired at 400°C for 1 hr; h is the intensity of the 10-Å peak; and b is the back-

[1] Department of Geology, University of Geology, Christchurch, New Zealand. Present address: Geology Department, University of Western Australia, Nedlands, Western Australia 6009, Australia.

[2] Department of Physics, University of Canterbury, Christchurch, New Zealand.

[3] Department of Physics, University of Canterbury, Christchurch, New Zealand.

[4] Department of Geology, University of Canterbury, Christchurch, New Zealand.

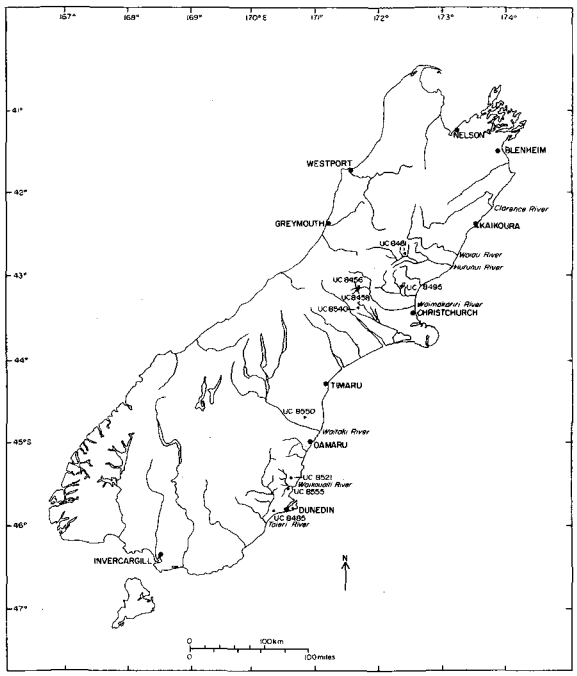

Figure 1. Location map for sampled outcrops, South Island, New Zealand, UC numbers refer to samples stored in the Geology Department, University of Canterbury, whence details on location and stratigraphy can be obtained.

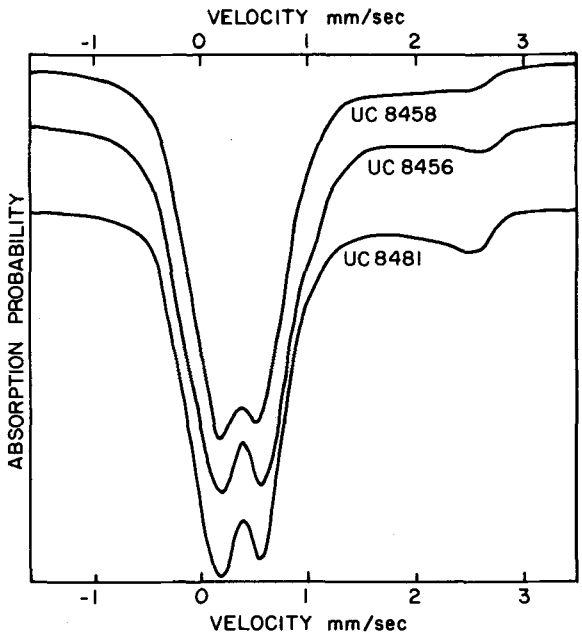

Figure 2. Mössbauer spectra of selected glauconites taken at room temperature. The curves are smoothed lines drawn through the data points; they are not fitted sets of peaks with Lorentzian shapes. Spectra taken at room temperatures are not used to determine the parameters of the Mössbauer peaks (see text). [All velocities are relative to natural Fe (U.S. National Bureau of Standards absorber No. 1541). No scale is given for the ordinate axis because with deblackened data the ordinate represents absorption probability which is dimensionless; the scale is the same for all samples.]

ground intensity (h and b have the same arbitrary length units). In combination, the disorder coefficient and the % expandable layers determine the crystallinity class of each glauconite sample (see Table 1).

Chemical analyses of all samples (see Table 2) were performed by X-ray fluorescence techniques, and the total water content of the samples was determined as a percent weight loss on firing to 700°C for 1 hr, after correcting for Fe^{2+} oxidation. Differential thermal analysis curves for glauconite (Grim, 1968; McConchie and Lewis, 1978) show that essentially all dehydration and dehydroxylation ceased by this temperature and that structural changes took place at higher temperatures. The Fe^{2+}/Fe^{3+} ratio was determined from the Mössbauer spectra of the glauconites using relative peak areas; wet chemical methods were not used because if charge transfers occur in glauconites at room temperature, as suggested by the Mössbauer spectra taken in this study, then changes in the Fe^{2+}/Fe^{3+} ratio may occur during wet chemical analyses.

Mössbauer analysis

Specimens for Mössbauer analysis were prepared by grinding a subsample of the glauconite extract to <5 μm, mixing it with a boric acid binder to an iron concentration of 10 mg/cm^2, and pressing the mixture into a steel ring under a pressure of 1500 kg/cm^2. Further spectra were taken from subsamples of UC8458 which were pretreated as follows: (1) One subsample was leached by boiling in 10% HCl. (2) Another subsample, treated as in (1), was left standing for 1 month in a concentrated solution containing $^{57}Fe^{2+}$ and K^+.

Subsequent analyses employed a horizontally aligned Mössbauer apparatus with a linear drive system, used in a constant acceleration mode. The source used was Co^{57} in rhodium, with a line width of 0.108 mm/sec and an f (recoilless fraction) value of 0.78. Standardization was with respect to natural Fe at 298°K, and all isomer shifts are so reported in this paper. The background correction factor was determined using a 1.5×10^{-4} m thick Cu filter which absorbs all 6 KeV X-rays and all 14.4 KeV γ-rays while passing 95.25% of the 122 KeV and 136 KeV γ-rays. The spectra of all samples were recorded with the absorber temperature held at 80 ± 1°K using a Ricor (Type MCH-5) cryostat. In addition, the spectra of 4 samples (UC8456, UC8458, UC8481, and UC8521) were recorded with the absorber at room temperature.

The first stage of computer analysis of the raw data involved deblackening the data using the method of Dibar Ure and Flinn (1971) to remove the source line width; this process also removes distortions in peak

https://doi.org/10.1346/CCMN.1979.0270504 Published online by Cambridge University Press

Table 1. Morphological and crystallographic classification of the glauconites.

Sample No.[1]	Morphology[2]	Disorder coefficient[3]	Percent expandable layers	Class[4]	Crystallinity[5]
UC8456	V 5%, ZA 94%, pigmentary 1%	0.61	30	interlayered	2b (extremely disordered)
UC8458	L 90%, D 10%,	0.35	20	disordered	2a (moderately disordered)
UC8481	L trace, FA 70%, FB 30%	0.33	10	disordered	2a (moderately disordered)
UC8485	Z A/B 60%, L 10%, FA 25%, FB 5%	0.16	4	ordered (mineral)	1 (ordered)
UC8495	L 70%, D 10%, Z A/B 20%	0.75	45	interlayered	3 (interlayered)
UC8521	Z A/B 100%	0.16	20	ordered (mineral)	1 (ordered)
UC8540	L 50%, V trace, FA 40%, D 10%	0.39	4	disordered	2a (moderately disordered)
UC8550	L 30%, V 60%, FA 10%	0.85	30	interlayered	2b (extremely disordered)
UC8555	Z A/B 90%, L 1%, V 5%, D 1%, FA 3%	0.58	30	interlayered	2b (extremely disordered)

[1] See Figure 1 for sample locations.

[2] V = vermicular; L = lobate; FA = fragmentary glauconite subclass A; FB = fragmentary glauconite subclass B; ZA = spongy glauconite, cauliflower subclass; ZB = spongy glauconite, serrulate subclass; D = ovoid. Terminology of Triplehorn (1966) and McConchie (1978).

[3] For definition of the disorder coefficient (DC) see text.

[4] Crystallographic classification of the glauconites using the method of Burst (1958a).

[5] 1 = ordered; DC $\leq$ 0.25. 2a = moderately disordered; 0.25 < DC $\leq$ 0.5, % expandable layers < 40%. 2b = extremely disordered; DC > 0.5, % expandable layers < 40%. 3 = interlayered: % expandable layers > 40% (after McConchie, 1978).

amplitudes and areas caused by saturation. The resulting lines are narrower by about 0.1 mm/sec, and spectral resolution is thus greatly improved. In the second stage, ideal pairs of Lorentzian curves were fitted to the deblackened experimental data (Figure 4). The fitting program was designed to provide a minimum value for χ^2 but because the deblackening process applied a smoothing correction (see Dibar Ure and Flinn, 1971) and refined the raw data, the numerical value of χ^2 for the comparison of the experimental data and the fitted curves is not an adequate indicator of goodness of fit. Hence, goodness of fit must be determined by visual examination of the relationship between the deblackened experimental data and the fitted curves (see Figure 3). Finally, the deblackened experimental data and the calculated fit were plotted on a graph (Figure 4), and the computed curve parameters were tabulated (Table 3).

Table 2. Concentrations of major elements in the studied glauconites.

	Wt %									
Sample number	SiO_2	Al_2O_3	Total Fe as Fe_2O_3	MgO	CaO	K_2O	Na_2O	TiO_2	H_2O	Fe^{2+}/Fe^{3+}
UC8456	57.6	9.9	17.5	0.75	0.23	6.60	0.90	0.52	5.67	0.159
UC8458	53.2	4.3	25.6	1.21	0.63	8.34	0.40	0.13	5.28	0.244
UC8481	53.1	6.7	21.9	2.41	0.84	6.91	0.27	0.90	5.21	0.608
UC8485	54.5	4.0	23.6	0.89	0.09	7.81	0.45	0.30	6.20	0.016
UC8495	55.1	7.0	20.2	2.07	1.12	4.30	1.37	0.30	7.28	0.122
UC8521	53.2	6.7	24.6	0.41	0.25	6.02	0.72	0.41	6.58	0.007
UC8540	53.3	4.3	25.3	0.43	0.64	7.91	0.08	0.22	5.41	0.292
UC8550	50.2	5.4	28.6	0.11	0.75	6.72	0.25	0.33	7.23	0.072
UC8555	55.7	6.5	22.9	0.40	0.47	6.42	0.85	0.42	5.94	0.111

See Figure 1 for sample locations. All concentrations are expressed as weight % of the oxide. Weight ratios for Fe^{2+}/Fe^{3+} are determined from the Mössbauer spectra (see text).

https://doi.org/10.1346/CCMN.1979.0270504 Published online by Cambridge University Press

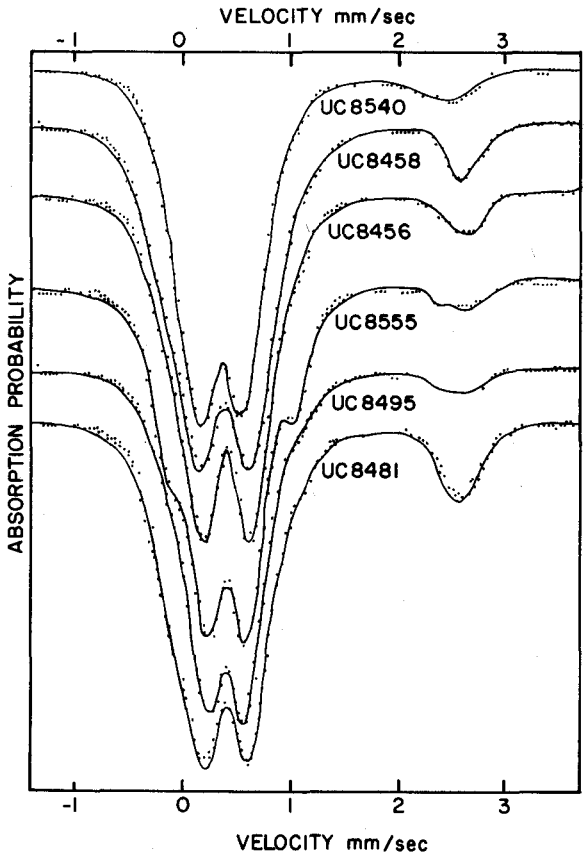

Figure 3. Mössbauer spectra of selected glauconites taken at 80°K with computer fitted curves. [All velocities are relative to natural Fe (U.S. National Bureau of Standards absorber No. 1541). No scale is given for the ordinate axis because with deblackened data the ordinate represents absorption probability which is dimensionless; the scale is the same for all samples.]

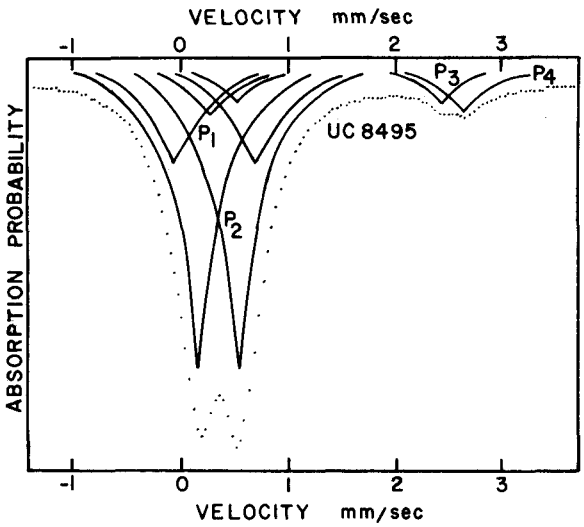

Figure 4. Mössbauer spectrum of sample UC8495 (deblackened data) showing individual quadrupole doublets as fitted to the deblackened data curves. For the parameters of the quadrupole doublets P_1, P_2, P_3, and P_4 see Table 3.

RESULTS

Effect of absorber temperature on peak resolution

Most previous Mössbauer work with glauconite (Hofmann *et al.*, 1967; Weaver *et al.*, 1967; Taylor *et al.*, 1968; Annersten, 1975; Raclavasky *et al.*, 1975) was carried out with the absorber at room temperature. These spectra showed, in addition to the major peaks, a region of continuous low intensity absorption (absorption shoulder) between approximately 1.0 and 2.5 mm/sec; the shoulder can not be satisfactorily fitted to peaks with Lorentzian form unless unrealistically high

Table 3. Peak parameters for Mössbauer spectra of glauconites, at 80°K.[1]

	P_1				P_2				P_3				P_4			
Sample	IS ± 0.01	QS ± 0.04	Γ ± 0.04	I ± 0.04	IS ± 0.01	QS ± 0.02	Γ ± 0.02	I ± 0.02	IS ± 0.02	QS ± 0.04	Γ ± 0.05	I ± 0.05	IS ± 0.02	QS ± 0.04	Γ ± 0.05	I ± 0.05
UC8456	0.41	0.97	0.43	0.11	0.46	0.43	0.40	0.39	1.66	1.76	0.17	0.03	1.42	2.72	0.41	0.07
UC8458	0.38	0.82	0.38	0.12	0.46	0.42	0.41	0.31	1.61	1.96	0.14	0.01	1.49	2.35	0.50	0.08
UC8481	0.44	1.27	0.21	0.21	0.48	0.44	0.45	0.30	1.40	2.36	0.55	0.05	1.32	2.65	0.50	0.15
UC8485	0.53	1.18	0.25	0.26	0.45	0.44	0.48	0.54	1.64	1.83	0.17	0.01	1.45	2.53	0.45	0.01
UC8495	0.39	0.75	0.51	0.10	0.46	0.38	0.39	0.34	1.55	1.93	0.18	0.03	1.53	2.36	0.52	0.04
UC8521	0.53	1.20	0.23	0.20	0.45	0.45	0.48	0.62	1.64	1.80	0.16	0.01	1.47	2.47	0.46	0.01
UC8540	0.38	0.69	0.39	0.15	0.42	0.36	0.35	0.25	1.56	1.84	0.37	0.02	1.44	2.14	0.58	0.06
UC8550	0.52	1.29	0.20	0.06	0.45	0.46	0.48	0.49	1.68	1.68	0.16	0.03	1.35	2.75	0.25	0.05
UC8555	0.52	1.25	0.25	0.16	0.47	0.41	0.43	0.55	1.56	1.90	0.16	0.04	1.38	2.81	0.39	0.07
Mean	0.46	1.04	0.32	N.A.	0.46	0.42	0.43	N.A.	1.59	1.90	0.23	N.A.	1.43	2.53	0.45	N.A.
Std. Dev'n	0.07	0.24	0.11		0.02	0.03	0.05		0.09	0.19	0.14		0.07	0.22	0.10	

[1] See Figure 1 for sample locations. P_1, P_2, P_3, P_4 represent quadrupole doublets. Isomer shift (IS), quadrupole splitting (QS), and half-height line width (Γ) are in mm/sec. Intensity (I) is absorption probability.

https://doi.org/10.1346/CCMN.1979.0270504 Published online by Cambridge University Press

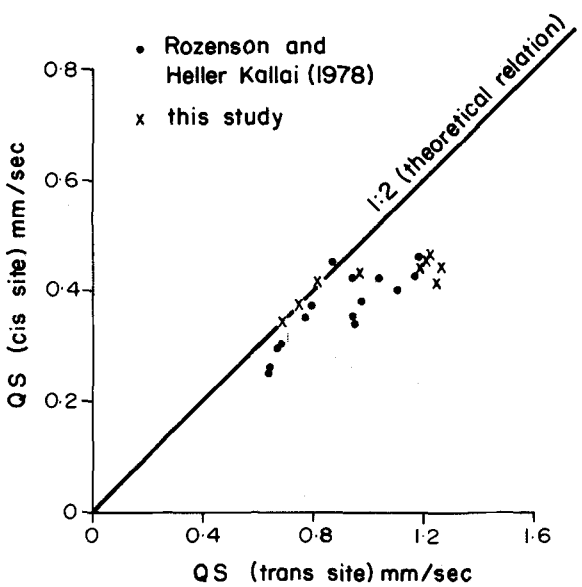

Figure 5. Scatter plot showing the relationship between QS values for Fe^{3+} in cis and trans octahedral sites in the glauconites studied.

line widths are used. Spectra taken under the same conditions in this study (Figure 2) showed the presence of a similar absorption shoulder. By analogy with patterns found for ilvaite (Heilman *et al.*, 1977) and some synthetic spinels (Lotgering and Van Diepen, 1976), the flat shoulder suggests that some Fe in glauconite may have a variable oxidation state. To test this possibility, the analyses were repeated with the absorber held at 80 ± 1°K. At this lower temperature the absorption shoulder disappeared, and the peaks showed a more symmetrical configuration (see Figure 3) as previously noted by Rolf *et al.* (1977). The exceptionally high line widths of 1.37 mm/sec (noted by Rozenson and Heller-Kallai, 1978) for some Fe^{2+} doublets also disappeared at low temperature, because they represent the absorption shoulder and not a true absorption peak. The difference in spectral form which resulted from the change in absorber temperature is very marked and may explain the observation that while a good fit can be obtained for deblackened data recorded at the lower temperature, the same is not true for data recorded at room temperature. Because the presence of the absorption shoulder on spectra taken with the absorber at room temperature prevents good fits being obtained for the Fe^{2+} peaks, the parameters for peaks fitted to room temperature spectra are of questionable interpretative value and are excluded from the following discussion.

It thus appears that at room temperature an Fe^{2+} ion may lose an electron to an adjacent Fe^{3+} ion, resulting in a reversal of their oxidation states, but that such charge transfer does not occur at 80°K. It is possible that the absorption shoulder observed in room-temperature Mössbauer spectra of glauconite is due to some form of temporary relocation of electrons (from Fe ions), without actual transfer to other Fe ions. However, electron transfer between ions with differing oxidation states is the more likely explanation because: (1) the zone between adjacent octahedral cations has the lowest electron density, hence the lowest energy barrier to electron movement (oxygens of the octahedral and tetrahedral sheets provide a charge barrier to intersheet electron movement); and (2) Fe^{2+} ions can be oxidized to Fe^{3+} during or after being taken into the glauconite crystal (see below), a process which must involve electron transfer. It is also probable that charge transfers between Fe^{3+} and Fe^{2+} can occur without having a significant effect on the Mössbauer spectra (e.g., Rozenson and Heller-Kallai, 1976), commonly where the Fe^{2+}/Fe^{3+} ratio is particularly high or particularly low (cf. Figure 1, Lotgering and Van Diepen, 1976) and/or the total Fe content in the absorber is low. An investigation of the rate of charge transfer and the energy involved, using Mössbauer, conductivity and magnetic susceptibility methods over a range of temperatures, can usefully form the basis of future work.

Interpretation of the Mössbauer spectra

On the Mössbauer spectra of glauconite recorded at 80 ± 1°K four pairs of peaks are evident (see Figure 4 and Table 3), all of which relate to Fe in octahedral coordination (Bancroft, 1973). The two pairs with larger IS and QS values can be identified as Fe^{2+} (Bancroft *et al.*, 1967), whereas the two pairs with smaller IS and QS values can be related to Fe^{3+}.

The presence of two quadrupole doublets for Fe in each oxidation state indicates clearly that there is more than one possible atomic configuration involving octahedral iron in glauconite. Each unit cell of a phyllosilicate mineral has three possible octahedral sites: one M(1) site with hydroxyl groups arranged in a trans configuration, and two M(2) sites with the hydroxyl groups arranged in a cis configuration (Rolf *et al.*, 1977; Rozenson and Heller-Kallai, 1978). In an ideal structure the two M(2) sites are equivalent, while the M(1) site is slightly larger (Rozenson and Heller-Kallai, 1977). The differences between these two sites are considered to be responsible for the existence of the two Fe^{3+} and two Fe^{2+} doublets observed in the Mössbauer spectra of glauconite (Rolf *et al.*, 1977; Rozenson and Heller-Kallai, 1978).

The quadrupole splitting (QS) in a Fe^{57} Mössbauer spectrum is given by Bancroft (1973) as

$$QS = \tfrac{1}{2}e^2qQ[1 + (n^2/3)]^{1/2}$$

where eq = Vzz = − the Z component of the electric field gradient (EFG) at the nucleus; n = (Vxx − Vyy)/Vzz and is the asymmetry parameter; and eQ is the nuclear quadrupole moment. Ingalls (1964) showed that q can be divided into two terms:

https://doi.org/10.1346/CCMN.1979.0270504 Published online by Cambridge University Press

$$q = (1 - R)q_{valence} + (1 - \gamma_\infty)q_{lattice}$$

of which the first gives the contribution to the EFG from the Mössbauer atom's own electrons and the second is due to surrounding charges on the lattice.

For a spherically symmetric ion (such as Fe^{3+} in an octahedral site with electronic configuration $t_{2g}^3e_g^2$), the $q_{valence}$ term is zero, and the quadrupole splitting arises solely from the field of the surrounding ions, modified by the Sternheimer antishielding factor γ_∞. In these circumstances Bancroft (1973) showed that for Fe^{3+} the magnitude of q at an octahedrally coordinated trans M(1) site is twice that for a cis M(2) site, and that η = 0 for both. Hence P_1 (see Table 3) is produced by octahedral Fe^{3+} in the trans M(1) configuration, while P_2 is produced by octahedral Fe^{3+} in the cis M(2) configuration. This assignment agrees with that of Rozenson and Heller-Kallai (1978), but is the reverse of that of Rolf *et al.* (1977).

With respect to the relative QS values for octahedral Fe^{3+}, a plot of QS M(1) against QS M(2) deviates markedly from the theoretical 2:1 ratio when QS M(2) is approximately 0.5 mm/sec (Figure 5). The precise reason for this deviation is not at present known; it could be due to the development of a π-bonding component in some samples, or it could result from changes in lattice distortion due to other factors. Although a smaller IS reflects a greater covalent contribution to the ligand bond (Rozenson and Heller-Kallai, 1977), there is no apparent correlation between IS and the extent of deviation from the theoretical line in Figure 5.

Two other features of the Fe^{3+} doublets are of particular interest.

(1) In an ideal unit crystal of glauconite the ratio of M(1) to M(2) sites is 1:2, whereas samples used in this study have a mean M(1) to M(2) occupancy ratio of 1:3. Bancroft (1973) showed that for silicate minerals, relative site populations are proportional to relative peak areas. Thus, it follows that octahedral Fe^{3+} in glauconite shows a strong preference for cis M(2) sites.

(2) The values of Γ for both M(1) and M(2) doublets are significantly greater than would be expected for an ideal crystal system. There may be a contribution to peaks assigned to octahedral Fe^{3+} in glauconite (particularly those with high Γ and QS values) from finely divided iron oxide/hydroxide inclusions which exhibit super-paramagnetic behavior. However, no evidence was found which suggests that iron oxides/hydroxides constitute >1% of any sample used in this study; other glauconites containing >1% iron oxides/hydroxides produced both 6-line and super-paramagnetic spectra but were excluded from further analyses. Hence, it appears that super-paramagnetic inclusions do not account for high Γ values, and some variation in the degree of site disorder is indicated. Because the mean value for Γ is greater for M(2) sites than for M(1) sites, it is likely that the M(2) site is the more readily distorted.

With respect to the Fe^{2+}, assignment of each doublet to a specific site is complicated by the facts that (1) Fe^{2+} is not a spherically symmetrical ion and hence $q_{valence}$ cannot be neglected, and (2) Fe^{2+} is significantly larger than Fe^{3+}. On a size basis it would be expected that Fe^{2+} would favor the larger trans site; however, preference may be shown for the more readily distorted cis site. Hogg and Meads (1970) suggested that most Fe^{2+} in dioctahedral micas occupies the trans sites; it is probable that the same relationship applies in the case of the glauconite (e.g., Rolf *et al.*, 1977) which, although predominantly dioctahedral, may have some trioctahedral character (McRae, 1972). Because most of the octahedral Fe^{2+} in glauconite is in the site with the larger QS (see Table 3), the present data suggest that the Fe^{2+} occurs preferentially in the trans M(1) site. If this conclusion is valid, then Fe^{2+} in glauconite shows a strong preference for the trans M(1) site; the mean ratio of peak areas for M(1) and M(2) is 4.9:1 (see Table 3). Hence, P_4 in Table 3 represents the larger QS trans site, whereas P_3 represents the smaller QS cis site. Rozenson and Heller-Kallai (1978) used a reversed assignment based on that of Annersten (1975), but the reasons for Annersten's original assignment are not clear. Resolution of the Fe^{2+} doublets is considerably inferior to that of the Fe^{3+} doublets, however, and assignment is thus tentative.

Assignment of the Fe^{2+} doublet with the larger QS to the trans site is supported by the observation that as the proportion of Fe^{3+} in the trans site increases, so does the proportion of Fe^{2+} in the site with the larger QS. Furthermore, as the proportion of octahedral Al^{3+} increases, so does the proportion of Fe^{3+} in the M(1) site and Fe^{2+} in the site with the larger QS, suggesting that octahedral Al^{3+} shows an even stronger preference for M(2) sites than does Fe^{3+}, and that its presence restricts the entry of Fe in either oxidation state to the M(2) site. (The ratio of total Fe to octahedral Al^{3+} may be correlated with the proportion of Fe, in each oxidation state, which occupies the M(1) site; for Fe^{3+} the correlation R = −0.78 and for Fe^{2+}, R = −0.62.) However, as with the assignment of the Fe^{2+} doublets, this suggestion is somewhat tentative.

The values for IS and QS vary somewhat between samples, although the standard deviation is not high; similar variance has also been reported by others (e.g., Rozenson and Heller-Kallai, 1978). The variance is probably related to differences in the degree of crystallographic disorder and proportions of expandable layers between the samples. However, variance is accentuated with Fe^{3+} in the trans site and Fe^{2+} in either site by the generally low intensity and poor resolution of these peaks.

Several workers (e.g., Thompson and Hower, 1975; Birch *et al.*, 1976) suggested that nonstructural Fe in glauconite is in part responsible for the wide variation in glauconite compositions. No evidence has been

found in this study to support this suggestion, however, because glauconites which showed evidence of oxidation were excluded from the analyses, it is possible that nonstructural Fe is present in such grains. Although the presence of tetrahedral Fe in glauconite has been suggested (Bentor and Kastner, 1965; Caillère and Lamboy, 1970; McRae, 1972), it was not detected during this study, nor has it been reported in other Mössbauer studies of glauconite (e.g., Annersten, 1975; Rolf *et al.*, 1977).

GLAUCONITE GENESIS

Glauconite forms almost exclusively in marine environments (McRae, 1972). Occurrences have been reported in nonmarine sediments (e.g., Keller, 1956; Parry and Reeves, 1966; McConchie and Lewis, 1978), but where glauconite occurs as discrete grains it may have been reworked from marine deposits (e.g., McConchie and Lewis, 1978), or the chemistry of the nonmarine solutions may have been very similar to that of marine waters (Parry and Reeves, 1966). A very low (to negative) sedimentation rate in the genetic environment is considered essential (e.g., Van Andel and Postma, 1954; Cloud, 1955; Burst, 1958b; McRae, 1972), and water depths equivalent to the neritic environment (immediately sublittoral to the upper part of the continental slope) are generally inferred (see McRae, 1972). A periodically agitated low energy environment appears to be necessary (Van Andel and Postma, 1954; McRae, 1972; Odin, 1975), but in many occurrences, current generated structures probably reflect reworking after the glauconite was formed (e.g., Ward and Lewis, 1975; McConchie, 1978; McConchie and Lewis, 1978). A pH of 7 to 8 (Fairbridge, 1967) and slightly reducing conditions (Eh < 0) are generally considered to be the most favorable (Cloud, 1955; Burst, 1958a; Fairbridge, 1967), although the reducing conditions may be confined to the immediate vicinity of the proto-glauconite (Burst, 1958a; Norris, 1964), while the overall conditions remain slightly oxidizing (Van Andel and Postma, 1954).

The association of authigenic glauconite with organic matter is well known (McRae, 1972); the organic matter may be involved in producing the required Eh conditions, and/or it may be involved in the degradation of phyllosilicate progenitors. However, too much organic matter may be as undesirable as too little, in that (1) chelation may limit the availability of Fe, (2) the Eh may become too negative, (3) an over-supply of organic acids may be able to degrade the glauconite faster than it can form, or (4) an abundance of organic sulphur may result in the formation of iron sulphides in preference to glauconite.

Whereas some glauconites appear to have precipitated in voids (e.g., within foraminiferal tests or interstitially in sediments), some replaces organic hardparts (see, Cayeux, 1916), and some formed as alteration products of silicate minerals such as feldspars (Carozzi, 1960), the glauconites used in this study appear to have formed from fine grained phyllosilicates aggregated as fecal pellets (McConchie, 1978; also see Takahashi and Yagi, 1929).

The first stage of glauconitization probably involves the degradation of an original phyllosilicate (Burst, 1958a, 1958b; Hower, 1961) with a loss of octahedral cations, either as a result of inorganic processes or as a result of organically controlled processes such as bacterial metabolism (Prather, 1905), and/or the passage of sediments through the guts of organisms (Pryor, 1975). It is also possible that the precursor material may have been an authigenic phyllosilicate with an incompletely developed crystal structure (Odin, 1975; Odin *et al.*, 1978).

Whatever the origin of the degraded phyllosilicates, they can be assumed to have had a high positive charge deficiency due to lack of sufficient structural cations in the octahedral layer. The charge deficiency is likely to have been temporarily balanced by highly mobile and readily available marine cations such as Mg^{2+}, K^{+}, Ca^{2+}, and Na^{+}, until such time as they were replaced by structural Fe. McConchie (1978) showed a negative correlation between total Fe and Mg ($R = -0.63$), and between total Fe + Al and Mg ($R = -0.82$) for 142 glauconites, suggesting that the dominant temporary stabilizing cation may have been Mg^{2+}.

Positive charge deficiencies due to the replacement of some tetrahedral Si^{4+} by Al^{3+} and the presence of some divalent cations in the octahedral layer, were balanced by interlayer cations (predominantly K^{+} in glauconite) which were not replaced by Fe during glauconitization. Because K^{+} and $Fe^{2+/3+}$ ions occupy entirely different lattice positions in glauconite and perform different functions, the reactions involving these two cations are probably independent (e.g., Bentor and Kastner, 1965; and Birch *et al.*, 1976), and occur at different times and rates (Foster, 1969), rather than simultaneously as suggested by Hower (1961).

Because virtually no potential phyllosilicate progenitor contains as much Fe as glauconite, the uptake of Fe must be the fundamental reaction in the glauconitization process. Biotite appears to be the only abundant phyllosilicate that may contain as much Fe as glauconite (Burst, 1958b), but most workers agree that only a small proportion of glauconites appear to have formed from biotite (Cayeux, 1916; Carozzi, 1960; Burst, 1958a, 1958b; Hein *et al.*, 1974; Odin, 1975).

Because Fe^{3+} is geochemically immobile in solution (James, 1966), the Fe is most likely to be taken up by the proto-glauconite as Fe^{2+}; even if some Fe^{3+} was present in solution, it would have been in proportionately low concentration. Fe^{2+} may enter (and leave) the degraded octahedral layer of the proto-glauconite by

ion exchange, depending on charge deficiencies in the crystal and equilibrium considerations. Once inside the degraded octahedral layer, however, the Fe^{2+} may lose an electron during bond formation and become 'fixed' as Fe^{3+}. The energy barrier to such a reaction would appear to be low (Burns, 1970), and the released electron may be moved out of the crystal structure by a series of charge transfer reactions, although this latter suggestion is wholly speculative at present. Once outside the glauconite crystal, the electron may be involved in reduction reactions, including the reduction of any Fe^{3+} which may be available. Since Fe^{2+} is eliminated within the lattice with the production of Fe^{3+}, the concentration gradient favors continued entry of Fe^{2+} from the surrounding solutions. However, it is not essential that all Fe^{2+} be oxidized in the proto-glauconite, and not all of it is (Figures 2, 3 and Table 3). Sufficient Fe^{2+} remains in the glauconite for the effects of electron exchange between octahedral Fe^{2+} and Fe^{3+} cations to be recorded in the ancient glauconites.

Experimental support for the above mechanism was obtained as follows: The Fe content of glauconite (UC8458) was reduced by approximately 10% by boiling it in 10% HCl and partially restored by soaking the leached mineral in a solution containing $^{57}Fe^{2+}$ and K^+ for 1 month.

The only iron available to the leached glauconite was in the Fe^{2+} oxidation state; nevertheless, the intensity of the Fe^{3+} peaks in subsequent Mössbauer spectra increased by approximately the same amount as the intensity of the Fe^{2+} peaks (i.e., 6–8%). Hence, it would appear that a degraded or partially degraded glauconite crystal structure can oxidize Fe^{2+} to Fe^{3+}. The results of this experiment do not imply that glauconitization is reversible (see Robert, 1972; Robert *et al.*, 1973) but they do suggest that the final Fe^{2+}/Fe^{3+} ratio in the glauconite may not be a true indicator of the Eh conditions in the genetic environment. Whether or not the crystal structure of other authigenic sedimentary minerals can induce changes to the Fe^{2+}/Fe^{3+} ratio in the manner described for glauconite is at present uncertain, although the possibility should be investigated. Although this experiment appears to support the model for glauconitization described herein, the possibility that the results obtained may have been due to other causes (e.g., changes in the mineral caused by the leaching process and not detected by Mössbauer or X-ray diffraction examination) cannot be totally discounted. However, because a negative Eh was maintained in the $^{57}Fe^{2+}$ solution it seems probable that the oxidation necessary to produce the increased octahedral Fe^{3+} content, must have taken place within the glauconite itself.

From the model proposed here for the glauconitization of degraded or incomplete phyllosilicate crystals, two principal factors appear to govern whether or not glauconitization will proceed, and if so, how far. (1) The Eh in the immediate vicinity of the degraded phyllosilicate must be negative (the Eh will depend on such factors as the organic matter content of the sediment and the amount of agitation in the genetic environment). (2) There must be an adequate supply of Fe to the proto-glauconite (the Fe supply will be affected by sedimentation rate and possibly pH). Other factors, such as water depth, will have only a secondary effect, insofar as they influence these more important controls.

CONCLUSIONS

The Mössbauer spectra of glauconites, taken with the absorber at 80°K, show the presence of 4 quadrupole doublets; the two with the smaller IS (see Table 3) are produced by octahedrally coordinated Fe^{3+}, and the two with the larger IS by octahedrally coordinated Fe^{2+}. The Fe^{3+} and Fe^{2+} occur in both trans M(1) and cis M(2) sites; Fe^{3+} shows a strong preference for the cis site whereas Fe^{2+} shows an even stronger preference for the trans site.

In spectra taken at room temperature, the precise position of the Fe^{2+} peaks is partly obscured by the presence of a broad absorption shoulder which extends from approximately 1.0 to 2.5 mm/sec. The shoulder is absent in spectra taken at 80°K and appears to be due to charge transfers between octahedral Fe^{3+} and adjacent Fe^{2+} in the glauconites at room temperature.

The first stage of genesis for many glauconites is likely the formation of a defective or degraded phyllosilicate crystal structure. The degraded progenitor, which may be an authigenic, or a detrital mineral degraded predominantly by the activity of marine organisms, will have a highly charged crystal structure which is temporarily stabilized by readily available cations such as K^+, Na^+, Ca^{2+}, and particularly Mg^{2+}. Iron enters this proto-glauconite as Fe^{2+} by ion exchange with the temporary stabilizing cations but is oxidized during bond formation to become octahedral Fe^{3+}. Because the Fe^{2+} is oxidized to Fe^{3+} and is essentially removed from the free ion system, the concentration of Fe^{2+} in the proto-glauconite remains sufficiently low as to permit further Fe^{2+} to enter as the system tends toward equilibrium. Electrons released during the oxidation of Fe^{2+} may escape from the proto-glauconite, possibly by a series of charge transfer reactions, and take part in reduction reactions in the surrounding environment. Not all Fe^{2+}, however, is oxidized to Fe^{3+} in the proto-glauconite, and the glauconitization process may be temporarily or permanently halted at any stage by unfavorable changes in the Eh of the genetic environment, termination of the supply of Fe, or the filling of all available octahedral sites by Fe.

ACKNOWLEDGMENTS

The University of Canterbury is thanked for Research Assistant Grant 78/2/18. Drs. S. Weaver (Ge-

ology Department, University of Canterbury) and M. Laird (New Zealand Geological Survey, Christchurch) critically reviewed the manuscript, and G. S. Odin (Pierre and Marie Curie University) constructively criticized various points. Ms. L. Leonard (Geology Department, University of Canterbury) drafted the figures.

REFERENCES

Annersten, H. (1975) A Mössbauer characteristic of ordered glauconite: *Neues Jahrb. Mineral. Monatsh.* **8,** 378–384.

Bancroft, G. M. (1973) *Mössbauer spectroscopy: An Introduction for Inorganic Chemists and Geochemists:* McGraw-Hill, New York, 252 pp.

Bancroft, G. M., Maddock, A. G., and Burns, R. G. (1967) Applications of the Mössbauer effect to silicate mineralogy—I. Iron silicates of known crystal structure: *Geochim. Cosmochim. Acta* **31,** 2219–2246.

Bentor, Y. K. and Kastner, M. (1965) Notes on the mineralogy and origin of glauconite: *J. Sediment. Petrology* **35,** 155–166.

Birch, G. F., Willis, J. P., and Rickard, R. S. (1976) An electron microprobe study of glauconites from the continental margin off the west coast of South Africa: *Mar. Geol.* **22,** 271–284.

Burns, R. G. (1970) *Mineralogical Applications of Crystal Field Theory:* Cambridge University Press, Cambridge, 224 pp.

Burst, J. F. (1958a) 'Glauconite' pellets: their mineral nature and applications to stratigraphic interpretations: *Amer. Assoc. Petrol. Geol. Bull.* **42,** 310–327.

Burst, J. F. (1958b) Mineral heterogeneity in 'glauconite' pellets: *Amer. Mineral.* **43,** 481–497.

Caillère, S. and Lamboy, M. (1970). Etude minéralogique de la glauconite du plateau continental au Nord-Ouest de l'Espagne: *C.R. Acad. Sci.* Ser. D. **270,** 2057–2060.

Carozzi, A. V. (1960) *Microscopic Sedimentary Petrology:* Wiley and Sons, New York, 485 pp.

Cayeux, L. (1916) *Introduction à l'Étude Pétrographique des Roches Sédimentaires: Glauconie:* Imprimerie Nationale, Paris, 241–252.

Cloud, P. E. (1955) Physical limits of glauconite formation: *Amer. Assoc. Petrol. Geol. Bull.* **39,** 484–492.

Dibar Ure, M. C. and Flinn, P. A. (1971) A technique for the removal of the 'blackness' distortion of Mössbauer spectra. in *Mössbauer Effect Methodology,* I. J. Gruverman, ed., **7,** 245–262.

Fairbridge, R. W. (1967) Phases of diagenesis and authigenesis. in *Diagenesis in Sediments,* G. Larsen and G. V. Chilingar, eds., Elsevier, Amsterdam, 19–91.

Foster, M. D. (1969) Studies of celadonite and glauconite: *U.S. Geol. Surv. Prof. Pap.* **614F,** 17 pp.

Grim, R. E. (1968) *Clay Mineralogy:* 2nd ed., McGraw-Hill, New York, 596 pp.

Heilman, I. U., Olsen, N. B., and Olsen, J. S. (1977) Electron hopping and temperature dependent oxidation states of iron in ilvaite studied by Mössbauer effect: *Physica Scripta* **15,** 285–288.

Hein, J. R., Allwardt, A. O., and Griggs, G. B. (1974) The occurrence of glauconite in Monterey Bay, California, diversity, origins and sedimentary environmental significance: *J. Sediment. Petrology* **44,** 562–571.

Hofmann, U., Fluck, E., and Kuhn, P. (1967) Mössbauer spectrum of iron in glauconite: *Angew. Chem. Int. Ed. Engl.* **6,** 561–562.

Hogg, C. S. and Meads, R. E. (1970) The Mössbauer spectra of several micas and related minerals: *Mineral. Mag.* **37,** 606–614.

Hower, J. (1961) Some factors concerning the nature and origin of glauconite: *Amer. Mineral.* **46,** 313–334.

Ingalls, R. (1964) Electric-field gradient tensor in ferrous compounds: *Phys. Rev.* **133A,** 787–795.

James, H. L. (1966) Chemistry of iron-rich sedimentary rocks: *U.S. Geol. Surv. Prof. Pap.* **440W,** 61 pp.

Keller, W. D. (1956) Glauconitic mica in the Morrison Formation, Colorado: *Clays & Clay Minerals* **5,** 120–127.

Lotgering, F. K. and Van Diepen, A. M. (1976) Electron exchange between Fe^{2+} and Fe^{3+} ions on octahedral sites in spinels studied by means of paramagnetic Mössbauer spectra and susceptibility measurements: *J. Phys. Chem. Solids* **38,** 565–572.

McConchie, D. M. (1978) Cretaceous and Lower Tertiary glauconite in the South Island of New Zealand. M.Sc. Thesis, Univ. Canterbury, New Zealand, 245 pp.

McConchie, D. M. and Lewis, D. W. (1978) Authigenic, perigenic and allogenic glauconites from the Castle Hill Basin, North Canterbury, New Zealand: *N.Z. J. Geol. Geophys.* **21,** 199–214.

McRae, S. G. (1972) Glauconite: *Earth Sci. Rev.* **8,** 397–440.

Norris, R. M. (1964) Sediments of the Chatham Rise: *New Zealand Oceanographic Inst. Mem.* **26,** 40 pp.

Odin, G. S. (1975) Les glauconies, constitution, formation, age: Thèse de Doctorat Sciences Naturelles, Univ. Pierre et Marie Curie, Paris, 250 pp.

Odin, G. S., Curry, D., and Hurziker, J. C. (1978) Radiometric dates from N.W. European glauconites and the Paleogene time scale: *J. Geol. Soc. London* **135,** 481–497.

Parry, W. T. and Reeves, C. C. (1966) Lacustrine glauconitic mica from pluvial Lake Mound, Lym, and Terry counties, Texas: *Amer. Mineral.* **51,** 229–235.

Prather, J. K. (1905) Glauconite: *J. Geol.* **13,** 509–513.

Pryor, W. A. (1975) Biogenic sedimentation and alteration of argillaceous sediments in shallow marine environments: *Geol. Soc. Amer. Bull.* **86,** 1244–1254.

Raclavasky, K., Sitek, J., and Lipka, J. (1975) Mössbauer spectroscopy of iron in clay minerals: *5th Int. Conf. Mössbauer Spec. Proc. Part II,* 368–371.

Robert, M. M. (1972) Transformation expérimentale de glauconites et d'illites en smectites: *C.R. Acad. Sci.* Ser. D **275,** 1319–1322.

Robert, M. M., Isambert, M., and Tessier, D. (1973) Etudes et premières interprétations de l'évolution des glauconites dans les sols: *C.R. Acad. Sci.* Ser. D. **277,** 1129–1132.

Rolf, R. M., Kimball, C. W., and Odom, I. E. (1977) Mössbauer characteristics of Cambrian glauconite, central U.S.A.: *Clays & Clay Minerals* **25,** 131–137.

Rozenson, I. and Heller-Kallai, L. (1976) Reduction and oxidation of Fe^{3+} in dioctahedral smectites. 1. Reduction with hydrazine and dithionite: *Clays & Clay Minerals* **24,** 271–282.

Rozenson, I. and Heller-Kallai, L. (1977) Mössbauer spectra of dioctrahedral smectites: *Clays & Clay Minerals* **25,** 94–101.

Rozenson, I. and Heller-Kallai, L. (1978) Mössbauer spectra of glauconite reexamined: *Clays & Clay Minerals* **26,** 173–175.

Takahashi, J. I. and Yagi, T. (1929) The peculiar mudgrains and their relation to the origin of glauconite: *Econ. Geol.* **24,** 838–852.

Taylor, G. L., Ruotsala, A. P., and Keeling, R. O. (1968) Analysis of iron in layer silicates by Mössbauer spectroscopy: *Clays & Clay Minerals* **16,** 381–391.

Thompson, G. R. and Hower, J. (1975) The mineralogy of glauconite: *Clays & Clay Minerals* **23,** 289–300.

Triplehorn, D. M. (1966) Morphology, internal structure, and origin of glauconite pellets: *Sedimentology* **6,** 247–266.

Van Andel, T. J. and Postma, H. (1954) Recent sediments of the Gulf of Paria: in *Reports of the Orinoco Shelf Expedition,* North Holland, Amsterdam, 245 pp.

Ward, D. M. and Lewis, D. W. (1975) Paleoenvironmental implications of storm scoured ichnofossiliferous Mid-Tertiary limestones, Waihao district, South Canterbury, New Zealand: *N.Z. J. Geol. Geophys.* **18,** 881–908.

Weaver, C. E., Wampler, J. M., and Pecuil, T. E. (1967) Mössbauer analysis of iron in clay minerals: *Science* **156,** 504–508.

(Received 7 February 1979; accepted 12 June 1979)

Резюме—Мессбауэровские спектры 9 образцов глауконита из верхне-меловых и нижне-третичных слоев Южного Острова Новой Зеландии имеют широкий выступ из-за низкой интенсивности абсорбции, продолжающейся между 1,0 и 2,5 мм/сек, когда абсорбер находится при комнатной температуре; выступ отсутсвует и в спектрах появляются острые пики, если абсорбер находится при 80°К. Эти данные свидетельствуют, что при комнатной температуре происходит перемещение электронов между близко лежащими ионами Fe^{3+} и Fe^{2+}. Низко-температурные спектры показывают, что все Fe в глауконитах находится в октаэдрической форме. Fe^{3+} и Fe^{2+} ионы встречаются в цис- и транс-местах; Fe^{3+} сильно предпочитает цис-места, в то время как Fe^{2+} еще более сильно предпочитает транс-места.

Частично изменчивое состояние окисления Fe в глауконите рассматривается в качестве геохимической модели для глауконизации деградированного или неполного исходного филлосиликата. Модель включает обмен Fe^{2+} на другие катионы, которые временно стабилизируют исходный филлосиликат, после чего следуют реакции перемещения зарядов Fe^{2+}–Fe^{3+}. Каждая реакция является следствием стремления системы к равновесию. Эта модель подтверждается наблюдением, что в искуственно выщелоченном глауконите увеличивается содержание Fe^{3+} и Fe^{2+}, если его поместить в раствор, содержащий только ион Fe^{2+}.

Resümee—Mössbauer-Spektren von 9 Glaukonitproben aus Schichten der Oberen Kreide und des Unteren Tertiär von der Südinsel Neuseelands zeigen eine breite Schulter hervorgerufen durch die Absorption bei niedriger Intensität zwischen 1,0 und 2,5 mm/sek, wenn der Absorber Raumtemperatur hat. Die Schulter fehlt, und scharfe Spitze treten im Spektrum auf, wenn der Absorber eine Temperatur von 80°K hat. Die Ergebnisse deuten darauf hin, daß ein Elektronenübergang zwischen benachbartem Fe^{3+} und Fe^{2+} bei Raumtemperatur stattfindet. Die Niedrigtemperaturspektren zeigen, daß sich im Glaukonit das gesamte Fe in oktaedrischer Koordination befindet. Fe^{3+}- und Fe^{2+}-Ionen kommen sowohl in cis- als auch in trans-Stellungen vor: Fe^{3+} vor allem in cis-Stellungen, während Fe^{2+} in noch stärkerem Maße die trans-Stellungen bevorzugt.

Der teilweise unterschiedliche Oxidationszustand des Fe im Glaukonit wird nach einem geochemischen Modell als Glaukonitisierung degradierter oder unvollständiger Vorläufer-Schichtsilikate interpretiert. Dieses Modell sieht den Austausch von Fe^{2+} gegen andere Kationen vor, wodurch vorübergehend der Vorläufer stabilisiert wird, gefolgt von Fe^{2+}–Fe^{3+} Ladungübertragenreaktionen. Jede Reaktion ist durch die Tendenz des Systems bestimmt, das Gleichgewicht zu erreichen. Dieses Modell wird durch die Beobachtung gestützt, daß bei künstlich ausgelaugten Glaukoniten sowohl der Fe^{3+}- als auch der Fe^{2+}-Gehalt steigt, wenn sie in eine Lösung kommen, die Fe nur in Form von Fe^{2+} enthält.

Résumé—Les spectres Mössbauer de 9 échantillons de glauconite des couches du crétacé supérieur et du tertiaire inférieur du Ile Sud de Nouvelle-Zélande contiennent une large bande à cause d'absorption de basse intensité continue entre 1,0 et 2,5 mm/sec lorsque l'absorbant est à température ambiante, cette large bande est absente et des sommets prononcés sont apparents dans les spectres pris avec l'absorbant à 80°K. Les données suggèrent que le transfert d'électrons se passe entre les ions adjacents de Fe^{3+} et Fe^{2+} à température ambiante. Les spectres de basse température indiquent que tout le Fe dans les glauconites est en coordination octahédrique. Les ions Fe^{3+} et Fe^{2+} se trouvent à la fois dans les sites cis et trans; Fe^{3+} montre une préférence marquée pour les sites cis alors que Fe^{2+} montre une préférence plus marquée encore pour les sites trans.

L'état d'oxidation partiellement variable de Fe dans la glauconite est interprété à l'aide d'un modèle géochimique pour la glauconitisation d'un progéniteur phyllosilicate dégradé ou incomplet. Le modèle comprend l'échange de Fe^{2+} pour d'autres cations qui stabilizent temporairement le progéniteur, suivi par les réactions de transfert de charge Fe^{2+}–Fe^{3+}. Chaque réaction resulte de la tendance du système vers un état d'équilibre. Le modèle est appuyé par l'observation que la glauconite artificiellement draînée augment à la fois son contenu de Fe^{3+} et Fe^{2+} lorsque placé dans une solution contenant Fe^{2+} comme seul ion Fe présent.